Evaluating the Dispatchable Capacity of Base Station Backup Batteries in Distribution Networks

Pei Yong, *Graduate Student Member, IEEE*, Ning Zhang, *Senior Member, IEEE*, Qingchun Hou, *Graduate Student Member, IEEE*, Yuxiao Liu, *Graduate Student Member, IEEE*, Fei Teng, *Member, IEEE*, Song Ci, *Senior Member, IEEE*, and Chongqing Kang, *Fellow, IEEE*

***Abstract*—Cellular base stations (BSs) are equipped with backup batteries to obtain the uninterruptible power supply (UPS) and maintain the power supply reliability. While maintaining the reliability, the backup batteries of 5G BSs have some spare capacity over time due to the traffic-sensitive characteristic of 5G BS electricity load. Therefore, the spare capacity is dispatchable and can be used as flexibility resources for power systems. This paper evaluates the dispatchable capacity of the BS backup batteries in distribution networks and illustrates how it can be utilized in power systems. The BS reliability model is first established considering potential distribution network interruptions and the effects of backup batteries. Then, the analytical formula of the BS availability index is derived with respect to batteries' backup duration. The dispatchable capacity of BS backup batteries is evaluated in different distribution networks and with differing communication load levels. Furthermore, a potential application, daily operation optimization, is illustrated. Case studies show that the proposed methodology can effectively evaluate the dispatchable capacity and that dispatching the backup batteries can reduce 5G BS electricity bills while satisfying the reliability requirement.**

***Index Terms*—Base station, 5G, backup battery, demand response, dispatchable capacity, distribution networks, reliability, availability.**

NOMENCLATURE

Symbols of Distribution System and Base Stations

n	Node index
N	Total number of nodes
m	Line index
M	Total number of lines
b	Base station index
B	Total number of base stations
ϕ^n_{base}	Set of base stations connected to node n
ϕ^n_{path}	Set of paths from root node to node n
ϕ^n_{line}	Set of lines that belong to paths in ϕ^n_{path}
$\lvert\phi^n_{line}\rvert$	Number of components in ϕ^n_{line}
T_b	Communication traffic of base station b
L_b	Power load of base station b
C_b	Backup battery installed energy capacity of base station b
R_b	Minimum reserved energy capacity of base station b
D_b	Backup duration of base station b
S_b	Power supply device rated power of base station b
$Avail^m_{line}$	Availability index of line m
$Avail^n_{node}$	Availability index of node n
$Avail^b_{base}$	Availability index of base station b
$\underline{SoC_b(t)}$	Battery SoC lower limit of base station b
$\overline{SoC_b(t)}$	Battery SoC upper limit of base station b
$\overline{p^c_b(t)}$	Battery charging limit of base station b
$\overline{p^d_b(t)}$	Battery discharging limit of base station b.

Symbols of Reliability modeling

t, τ, γ	Time index
$X^m_{line}(t)$	Stochastic process of line m
λ_m	Failure rate of line m
μ_m	Repair rate of line m
p^b_{ba}	Working probability of backup battery of base station b
q^b_{ba}	Failure probability of backup battery of base station b
$X^n_{node}(t)$	Stochastic process of node n
$X^n_{agg}(t)$	Stochastic process after aggregation
i, j	State index of $X^n_{agg}(t)$
δ^n_w	Set of working states of $X^n_{agg}(t)$
δ^n_f	Set of failure states of $X^n_{agg}(t)$
$\boldsymbol{A}^n_{agg}$	Transition density matrix of $X^n_{agg}(t)$
$\boldsymbol{P}^n_{agg}(t)$	Transition probability matrix of $X^n_{agg}(t)$
$\boldsymbol{p}^n(t)$	Probability vector of $X^n_{agg}(t)$
ω	Markov chain index of $X^n_{agg}(t)$
$S^n_{agg}(t)$	Semi-Markov process correspond to $X^n_{agg}(t)$

Manuscript received December 7, 2020; revised March 8, 2021; accepted April 17, 2021. Date of publication April 21, 2021; date of current version August 23, 2021. This work was supported in part by International (Regional) Joint Research Project of National Natural Science Foundation of China under Grant 52061635101; in part by S&T Major Project of Inner Mongolia Autonomous Region in China under Grant 2020ZD0018; and in part by the Scientific and Technical Project of State Grid: Research on Multi Energy Storage Optimal Allocation for the Efficient Utilization of High Penetration Renewable Energy. Paper no. TSG-01814-2020. *(Corresponding author: Ning Zhang.)*

Pei Yong, Ning Zhang, Qingchun Hou, Yuxiao Liu, Song Ci, and Chongqing Kang are with the State Key Laboratory of Power Systems, Department of Electrical Engineering, Tsinghua University, Beijing 100084, China, and also with the International Joint Laboratory on Low Carbon Clean Energy Innovation, Tsinghua University, Beijing 100084, China (e-mail: ningzhang@tsinghua.edu.cn).

Fei Teng is with the Department of Electrical and Electronic Engineering, Imperial College London, London SW7 2BU, U.K.

Color versions of one or more figures in this article are available at https://doi.org/10.1109/TSG.2021.3074754.

Digital Object Identifier 10.1109/TSG.2021.3074754

$\boldsymbol{h}^n_{agg}(t)$ Transition density matrix of $S^n_{agg}(t)$
$\boldsymbol{H}^n_{agg}(t)$ Transition probability matrix of $S^n_{agg}(t)$.

I. Introduction

A. Motivation

INFORMATION and communications technology (ICT) has extensively promoted economic and social development in recent years. Meanwhile, the energy consumption of ICT infrastructures, especially cellular wireless networks, is increasing rapidly [1]. The 5th-generation mobile networks (5G) provide high bandwidth, high capacity, and low latency communication [2], but will consume much more energy than previous technology. The reasons for this are twofold: for one thing, the rated power for a single 5G cellular base station (BS) is approximately three to four times as large as that of 4G [3]; for another, due to the decrease of the effective communication distance, more BSs should be deployed to ensure network coverage.

While increasing energy consumption, the rapid growth of 5G BSs also provides lots of potential flexibility resources from backup batteries. They are installed in BSs to provide uninterruptible power supply (UPS) and maintain the BS power supply reliability (usually represented by the availability index) at a required level. The availability index measures the steady-state probability that the BS is at work to provide communication services. For example, the Next Generation Mobile Networks (NGMN) Alliance requires the 5G BS availability index to reach 99.999% [4]. In the past, the backup batteries only provided UPS because the conventional BS power load is stable during a day and does not change with the communication traffic. However, the 5G BS power load is traffic-sensitive [5]: i.e., when the communication traffic changes during the day, the power load changes accordingly. Also, the minimum reserved energy capacity for availability maintenance changes with time. Therefore, in addition to the reserved capacity, the 5G BS backup batteries have some spare energy capacity over time due to the traffic-sensitive electricity load. The spare capacity is dispatchable (referred to as BS dispatchable capacity). Hence, the energy capacity backup batteries can be dynamically divided into two virtual parts: the first part is used to maintain the availability; the remaining part can be dispatched. Meanwhile, with the development of renewable energy [6], [7], flexibility resources are becoming increasingly important for power systems to balance the load and generation [8], [9]. The backup batteries with dispatchable capacity are available flexibility resources for power systems.

It is beneficial for both power systems and mobile operators to dispatch the backup batteries. For the power systems, these dispatchable batteries provide extra flexibility resources and can be used in peak shaving or frequency regulation, promoting renewable energy integration. For the mobile operators, the electricity bills could be reduced by dispatching the batteries' spare capacity to do temporal arbitrage or participate in the ancillary service market. As the total power consumption will increase rapidly with the development of 5G, electricity bills are becoming one of the most significant concerns for mobile operators [5]. Therefore, dispatching the backup batteries is a win-win situation for power systems and mobile operators.

B. Literature Review

One of the critical problems for the backup battery dispatch is to evaluate the minimum reserved energy capacity for availability maintenance during different time slots. The BS availability level is determined by both the distribution networks and the reserved battery energy capacity. Methods for distribution network reliability evaluation have been widely discussed [10]. Recent research mainly focuses on detailed modeling. For example, Arefi *et al.* [11] model the network reconfiguration and distributed generations; Timalsena *et al.* [12] consider the breaker failure; Li *et al.* [13] incorporate the postfault reconfiguration; Liu *et al.* [14] consider information link failures; Gautam *et al.* [15] model the momentary event; Jooshaki *et al.* [16] formulate the switching interruptions; Liu *et al.* [17] extend to the gas-electric distribution systems. However, these methods do not incorporate backup batteries into the model. If the reserved backup energy capacity can serve the BS during an interruption, the operation of the BS will not be influenced. Hence, the backup batteries can significantly improve the reliability. This characteristic is referred to as "time interval omission" in signal processing [18]. The "time interval omission" characteristic is incorporated in some reliability models. Zheng *et al.* [19] consider the characteristic in a single-unit Markov repairable system. Bao and Cui [20] generalize the research framework to series systems. In [21], Liu *et al.* study the interval availability with time interval omission. These models cannot consider the complex power supply situations in distribution networks.

C. Contributions

To our best knowledge, there still remains a lack of methods to evaluate the BS availability level while comprehensively considering the distribution network characteristics and the backup batteries. Consequently, the potential flexibility of backup batteries cannot be fully utilized. In this regard, we propose a framework to evaluate the BS dispatchable capacity. The BS reliability model is constructed considering the factors of distribution networks and the effects of backup batteries. In the model, the states of BSs rely on not only the distribution networks (which are usually treated as Markov models) but also the batteries' reserved energy. Therefore, the model is non-Markovian. Semi-Markov analysis is introduced to deduce the analytical formula for the BS availability index. According to the formula, we further calculate the minimum backup duration for the availability requirement. Then, the BS dispatchable capacity is evaluated. An application case of the BS dispatchable capacity is constructed to validate the proposed method. The contributions are listed as follows:

1) An analytical reliability evaluation method based on semi-Markov analysis is proposed to calculate the BS availability index in distribution networks. The method considers the effects of backup batteries for the first time. The non-Markovian property brought by the backup batteries is effectively handled.

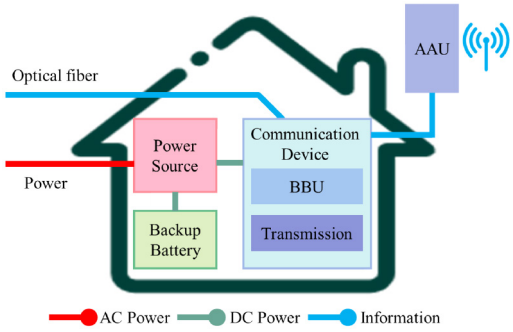

Fig. 1. Basic components of a 5G base station.

2) The BS dispatchable capacity is evaluated considering the availability requirement. The evaluation obtains the range in which the BS backup batteries can be charged and discharged while maintaining the required availability level.
3) The potential flexibility of BS backup batteries is explored. In this paper, an application of the BS dispatchable capacity is illustrated: the backup batteries are dispatched to reduce the BS operation cost.

D. Paper Organization

The remainder of this paper is organized as follows. Section II proposes the problems and the solution framework. Section III constructs the reliability model of the load points and the BSs. In Section IV, the method for evaluating the BS availability is proposed based on semi-Markov analysis. The BS dispatchable capacity is evaluated in Section V. Case studies are conducted in Section VI, and Section VIII draws the conclusion.

II. Problem Statement and Framework

The basic components of a 5G BS are illustrated in Fig. 1, which can be divided into the communication part and the power supply part. The power supply part is mainly composed of power sources (power electronic devices) and backup batteries. The power sources are the interface to the AC distribution networks and convert the power into DC. The backup batteries are prepared for distribution network interruptions. When an interruption occurs, the communication device power would be supplied by the backup batteries until the distribution networks are restored.

The 5G BS power load is traffic-sensitive and can be divided into two parts: the first part is fixed, and the second part is proportional to the communication traffic [22]:

$$L_b(t) = \alpha_b + \beta_b T_b(t) \tag{1}$$

where $L_b(t)$ is the power load, $T_b(t)$ is the communication traffic, and α_b and β_b are the coefficients. The power load changes with the communication traffic, so the minimum reserved energy capacity to provide UPS changes over time (shown in Fig. 2).

In this paper, we dynamically divide the backup battery energy capacity into two virtual parts: the first part is reserved

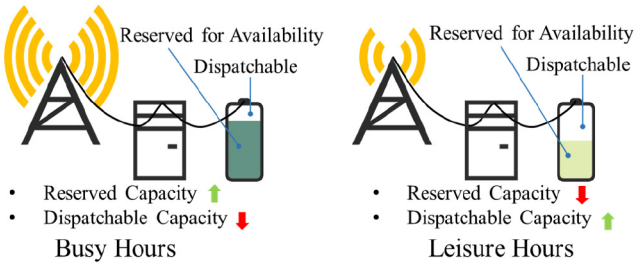

Fig. 2. Reserved and dispatchable capacity of backup batteries at different hours.

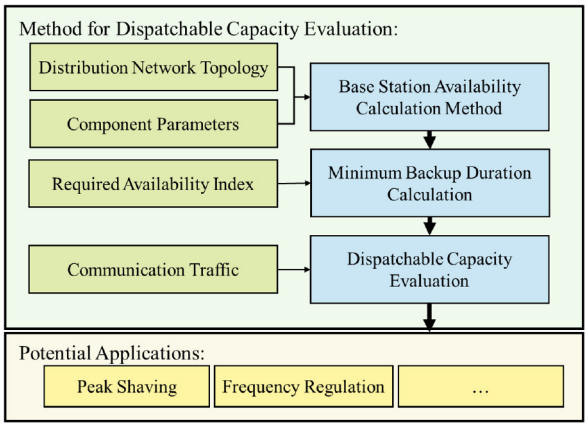

Fig. 3. Proposed framework for dispatchable capacity evaluation.

to maintain the availability; the remainder is dispatchable. It is necessary to evaluate the minimum reserved energy capacity $R_b(t)$ for the availability requirement so that the dispatchable capacity can be determined. $R_b(t)$ is calculated by the power load $L_b(t)$ and the backup duration D_b:

$$R_b(t) = \int_t^{t+D_b} L_b(\tau)d\tau \tag{2}$$

The value of backup duration D_b influences the BS availability index. A longer backup duration indicates that the BS is more robust to distribution network interruptions. Thus, the BS availability index increases.

However, BS availability index calculation is a great challenge because of two aspects. The well-developed Markov models cannot be used since the characteristics of backup batteries cause failure of the Markov property. An evaluation method considering non-Markovian characteristics is needed. Moreover, the method ought to be analytical. Since the availability requirement is always near 100% (99.999% for NGMN [4]), sampling-based methods would exhibit poor performances.

The proposed framework of this paper is shown in Fig. 3. First, the BS reliability model is constructed. The distribution network topology is modeled as a graph, and the components of the distribution network are modeled using Markov repairable models. The state of the BS is expressed as a stochastic process. Based on the stochastic process modeling, the working probability of the BS is studied to deduce the availability index. Semi-Markov analysis is applied to overcome the non-Markovian property caused by the backup batteries. The analytical formula to calculate the

BS availability index is established. Then, the backup duration D_b for the availability requirement can be estimated using the analytical formula. After this, the BS dispatchable capacity is evaluated using Eq. (1) and (2). This paper also illustrates the proposed method's effectiveness in an application case: dispatching the batteries to participate in the daily optimization.

III. Base Station Reliability Modeling in Distribution Networks

BSs' power load can be supplied by either the distribution networks or the backup batteries, so uncertainties from two aspects are considered. For the former aspect, we model the studied distribution network as a graph. Each feeder section, transformer, or tie-line is modeled as a line of the graph. The failures of lines in the graph are considered as Markov repair models. For the latter aspect, we introduce the backup battery failure probabilities to the proposed method.

A. Assumptions and Distribution Networks Modeling

According to the IEEE Standard [23], reliability events in distribution networks can be divided into momentary and sustained (permanent) interruptions. Momentary interruptions last 1 or 5 minutes and can be overcome by the BS backup batteries. Thus, we only consider the sustained interruptions caused by the distribution network component faults.

Here are some assumptions in the reliability modeling of distribution networks:

1) The protection equipment and the switches in the network are reliable.
2) After a fault, tie switches can change from opened status to closed status to transfer load points to other feeders and minimize the fault's influence.
3) The fault isolation and load transfer time is shorter than the battery backup duration of the BS.
4) The momentary faults are neglected.

It should be noted that we do not incorporate the locations or types of protection devices into the modeling for simplicity. However, the proposed framework and analysis methodology are applicable for detailed models (e.g., the model in [24]).

The studied distribution network is represented by a graph structure. Load points are modeled as nodes; feeder sections, transformers and tie-lines are modeled as lines. In particular, the main grid is modeled as the root node.

B. Reliability Modeling of Lines

The failure of feeder sections, transformers and tie-lines in the distribution networks influence the power supply of load points and BSs. They (represented as line) are modeled using the continuous-time Markov repair model [25].

Definition 1: Line m's state is modeled as a continuous-time Markov process $\{X^m_{line}(t), t \geq 0\}$. The state space is defined as:

$$X^m_{line}(t) = \begin{cases} 0 & \text{line } m \text{ in failure state at time } t \\ 1 & \text{line } m \text{ in working state at time } t \end{cases} \quad (3)$$

This Markov process is homogeneous with failure rate λ_m and repair rate μ_m.

C. Reliability Modeling of Load Points

As per the description mentioned above, if there is an alternative power supply path after a sustained interruption, tie switches will be operated to transfer the studied load point to other feeders [24]. According to the assumptions, this kind of restorable interruptions can be omitted. Therefore, the states of the nodes (representing load points) are defined as follows.

Definition 2: Node n's state is modeled as a continuous-time stochastic process $\{X^n_{node}(t), t \geq 0\}$. The state space is defined as:

$$X^n_{node}(t) = \begin{cases} 0 & \text{node } n \text{ is cut off at time } t \text{ and cannot be restored by tie switch operations} \\ 1 & \text{otherwise.} \end{cases} \quad (4)$$

D. Reliability Modeling of Backup Batteries

Each BS is equipped with a backup battery module. The backup batteries' potential failures also influence the BS power supply. The backup batteries are represented as two-state models.

Definition 3: The backup battery of BS b has two states: the working state and the failure state. The working probability is p^b_{ba}; the failure probability is $q^b_{ba} = 1 - p^b_{ba}$.

E. Reliability Modeling of Base Stations

For BS b connected to node n, if node n is available, BS b' power load can be supplied by the distribution network. Otherwise, the backup battery ought to supply BS b's devices. In this case, if the backup battery of BS b is working, and the outage time of node n is shorter than battery backup duration, BS b is not influenced by the network interruptions. Thus, BSs are represented as two-state models.

Definition 4: BS b (connected to node n) has two states: the working state and the failure state. There are two situations that BS b is in the working state. Situation 1: node n is available. Situation 2: node n is out of service, outage time is shorter than battery backup duration, and the backup battery of BS b is working.

IV. Analytical Model for Base Station Availability Calculation

In this section, an analytical method is proposed to calculate the availability index. According to the modeling in Section III, we first derive the node availability indices based on Markov analysis. Then, the analytical formula to calculate the BS availability indices is deduced based on semi-Markov analysis. Furthermore, approximations and simplifications are proposed for engineering applications.

A. Availability of Load Points

According to Definition 2, for a given node n, if there is an available path from the root node (main grid) to node n, it is in the working state. The available path means that all lines of the path are in the working state at time t. Therefore, we search for all possible paths from the root node to node n

using the Depth First Search (DFS) algorithm [26]. We denote the set of all paths as ϕ^n_{path}. We denote the set of the lines that belong to at least one path in ϕ^n_{path} as ϕ^n_{line}.

As analyzed above, node n's state depends only on the states of the lines in ϕ^n_{line}. Each line corresponds to a Markov process as defined in *Definition 1*. We aggregate the Markov processes of lines in ϕ^n_{line} to form a new Markov process.

Definition 5: The Markov process $\{X^n_{agg}(t), t \geq 0\}$ is the aggregation of the Markov processes of lines in ϕ^n_{line}. The state space can be expressed as the binary code $x_1x_2\cdots x_{|\phi^n_{line}|}$, and the m-th bit represents the state of the m-th line in ϕ^n_{line} at time t.

$X^n_{agg}(t)$'s state space is divided into two categories: the working set δ^n_w and the failure set δ^n_f. For every state of $X^n_{agg}(t)$, we check whether node n is working or failure according to the path set ϕ^n_{path}. If node n is working, the state is included in δ^n_w; otherwise, it is included in δ^n_f. For convenience of the following analysis, the states are indexed with the following rule: the working states are indexed from 1 to $|\delta^n_w|$, and the failure states are indexed from $|\delta^n_w|+1$ to $|\delta^n_w|+|\delta^n_f|$.

The transition probability density matrix $\boldsymbol{A}^n_{agg}$ of $X^n_{agg}(t)$ can be constructed as follows [27]:

1) $\boldsymbol{A}^n_{agg}(i,j) = \lambda_m (i \neq j)$: if the binary codes of state i and j are equal, except for the m-th bit. The m-th bit of state i is 1; the m-th bit of state j is 0.
2) $\boldsymbol{A}^n_{agg}(i,j) = \mu_m (i \neq j)$: if the binary codes of state i and j are equal, except for the m-th bit. The m-th bit of state i is 0; the m-th bit of state j is 1.
3) $\boldsymbol{A}^n_{agg}(i,j) = 0 (i \neq j)$: other situations.
4) $\boldsymbol{A}^n_{agg}(i,i) = -\sum_{i \neq j} \boldsymbol{A}^n_{agg}(i,j)$.

The transition probability matrix $\boldsymbol{P}^n_{agg}(t)$ and the probability vector $\boldsymbol{p}^n(t)$ of $X^n_{agg}(t)$ are defined as follows:

$$\boldsymbol{P}^n_{agg}(t)(i,j) = Prob\Big(X^n_{agg}(t) = j | X^n_{agg}(0) = i\Big) \tag{5}$$

$$\boldsymbol{p}^n(t)(i) = Prob\Big(X^n_{agg}(t) = i\Big) \tag{6}$$

The relationship between the $\{X^n_{node}(t), t \geq 0\}$ and the $\{X^n_{agg}(t), t \geq 0\}$ is that: $X^n_{node}(t) = 1$ if and only if $X^n_{agg}(t)$ is in the working states. Thus, $X^n_{node}(t)$'s working probability can be expressed as:

$$Prob\big(X^n_{node}(t) = 1\big) = \sum_{i \in \delta^n_w} \boldsymbol{p}^n(t)(i) \tag{7}$$

We calculate $X^n_{node}(t)$'s working probability using Eq. (7), and let $t \to \infty$ to obtain load point n's availability index. The derivation details can be found in Appendix A. The result is:

$$Avail^n_{node} = \boldsymbol{p}^n(0) \cdot exp(\boldsymbol{A}^n_{agg}\infty) \cdot \begin{bmatrix} \boldsymbol{1}_{|\delta^n_w| \times 1} \\ \boldsymbol{0}_{|\delta^n_f| \times 1} \end{bmatrix} \tag{8}$$

where $exp(\boldsymbol{A}^n_{agg}\infty)$ is defined as $\lim_{t\to\infty} exp(\boldsymbol{A}^n_{agg}t)$.

B. Availability of Base Stations

As in *Definition 4*, BS b is at work under two situations. *Situation 1* is evaluated in Section IV-A, while *Situation 2* is analyzed focusing on the Markov process $\{X^n_{agg}(t), t \geq 0\}$. This situation occurs if and only if $X^n_{agg}(t)$ jumps from the working set δ^n_w to the failure set δ^n_f at time $t-\gamma$ ($\gamma \leq D_b$) and remains in the failure set δ^n_f until t; meanwhile, the backup battery is working. Because of the time interval γ, the Markovian property no longer holds. We analyze the probability of *Situation 2* with three steps.

1) Step 1 [Calculate the probability density that $X^n_{agg}(t)$ jumps from the working set δ^n_w to the failure set δ^n_f at time $t-\gamma$ ($\gamma \leq D_b$)]: We divide the transition density matrix $\boldsymbol{A}^n_{agg}$ and the transition probability matrix $\boldsymbol{P}^n_{agg}(t)$ into four parts:

$$\boldsymbol{A}^n_{agg} = \begin{bmatrix} \boldsymbol{A}^n_{ww} & \boldsymbol{A}^n_{wf} \\ \boldsymbol{A}^n_{fw} & \boldsymbol{A}^n_{ff} \end{bmatrix} \tag{9}$$

$$\boldsymbol{P}^n_{agg}(t) = \begin{bmatrix} \boldsymbol{P}^n_{ww}(t) & \boldsymbol{P}^n_{wf}(t) \\ \boldsymbol{P}^n_{fw}(t) & \boldsymbol{P}^n_{ff}(t) \end{bmatrix} \tag{10}$$

$\boldsymbol{A}^n_{wf}$ represents the probability density that $X^n_{agg}(t)$ jumps from the working set δ^n_w to the failure set δ^n_f; $\boldsymbol{P}^n_{ff}(t)$ represents the probability that $X^n_{agg}(t)$ only remains in the failure set δ^n_f and does not enter the working set δ^n_w in time $[0, t]$.

Thus, the probability density that $X^n_{agg}(t)$ jumps form the working set δ^n_w to the failure set δ^n_f at time $t-\gamma$ can be expressed as follows:

$$\boldsymbol{p}^n(t-\gamma) \cdot \begin{bmatrix} \boldsymbol{I}_{|\delta^n_w| \times |\delta^n_w|} \\ \boldsymbol{0}_{|\delta^n_f| \times |\delta^n_w|} \end{bmatrix} \cdot \boldsymbol{A}^n_{wf} \tag{11}$$

2) Step 2 [Calculate the probability that $X^n_{agg}(t)$ remains in the failure set δ^n_f from $t-\gamma$ until t]: A semi-Markov process based on $X^n_{agg}(t)$ is introduced to consider the time interval.

Definition 6: For the Markov process $\{X^n_{agg}(t), t \geq 0\}$, a Markov chain starting from $t = 0$ is expressed as $\{X^n_{agg,0}, X^n_{agg,1}, X^n_{agg,2}, \ldots, X^n_{agg,\omega}, \ldots,\}$ and the Markov chain jump moments are $\{t_0, t_1, t_2, \ldots, t_\omega, \ldots,\}$. The inter-arrival duration is $\tau_w = t_{w+1} - t_w$. The corresponding semi-Markov process is $\{S^n_{agg}(t), \tau\}$, where $S^n_{agg}(t) = X^n_{agg,\omega}$ and $\tau = t - t_\omega$.

The details of the semi-Markov process can be referred to in [28]. The transition probability matrix $\boldsymbol{H}^n_{agg}(\tau)$ of the semi-Markov process is defined as:

$$\boldsymbol{H}^n_{agg}(\tau)(i,j) = Prob\Big(X^n_{agg,\omega+1} = j, \tau_\omega \leq \tau | X^n_{agg,\omega} = i\Big) \tag{12}$$

where τ represents the time interval between two jumps of the Markov chain. The transition density matrix $\boldsymbol{h}^n_{agg}(\tau)$ of the semi-Markov process is defined as:

$$\begin{aligned} &\boldsymbol{h}^n_{agg}(\tau)(i,j)\ d\tau \\ &= Prob\Big(X^n_{agg,\omega+1} = j, \tau \leq \tau_\omega < \tau + d\tau | X^n_{agg,\omega} = i\Big) \end{aligned} \tag{13}$$

where $\boldsymbol{h}^n_{agg}(\tau)(i,j)$ represents the probability density that the Markov chain jumps into the state i, remains for τ, and jumps into state j in between τ and $\tau + d\tau$.

It should be noted that $\boldsymbol{H}^n_{agg}(\tau)$ and $\boldsymbol{h}^n_{agg}(\tau)$ are independent of the jumping time t_w and are only determined by the time interval τ because of $X^n_{agg}(t)$'s Markov property.

Similar to Eq. (9), $\boldsymbol{H}^n_{agg}(\tau)$ and $\boldsymbol{h}^n_{agg}(\tau)$ can be divided into four parts:

$$\boldsymbol{h}^n_{agg}(\tau) = \begin{bmatrix} \boldsymbol{h}^n_{ww}(\tau) & \boldsymbol{h}^n_{wf}(\tau) \\ \boldsymbol{h}^n_{fw}(\tau) & \boldsymbol{h}^n_{ff}(\tau) \end{bmatrix} \tag{14}$$

$$\boldsymbol{H}^n_{agg}(\tau) = \begin{bmatrix} \boldsymbol{H}^n_{ww}(\tau) & \boldsymbol{H}^n_{wf}(\tau) \\ \boldsymbol{H}^n_{fw}(\tau) & \boldsymbol{H}^n_{ff}(\tau) \end{bmatrix} \tag{15}$$

$\boldsymbol{h}^n_{fw}(\tau)$ represents the probability density that the Markov chain jumps into the failure set δ^n_f, remains for τ, and jumps into the working set δ^n_w in between τ and $\tau + d\tau$; $\boldsymbol{H}^n_{fw}(\tau)$ represents the probability that the Markov chain jumps into the failure set δ^n_f, remains shorter than τ, and jumps into the working set δ^n_w.

Thus, the probability that the Markov chain jumps into the failure set δ^n_f and remains longer than γ is:

$$\boldsymbol{H}^n_{fw}(\infty) - \boldsymbol{H}^n_{fw}(\gamma) \tag{16}$$

where $\boldsymbol{H}^n_{fw}(\infty)$ is defined as $\lim_{t\to\infty} \boldsymbol{H}^n_{fw}(t)$.

The derivation details of $\boldsymbol{h}^n_{fw}(\tau)$ and $\boldsymbol{H}^n_{fw}(\tau)$ can be found in Appendix B.

3) Step 3 [Combine Step 1 and Step 2 to Obtain the Probability]: According to Eq. (11) and Eq. (16), the probability density that $X^n_{agg}(t)$ jumps from the working set δ^n_w to the failure set δ^n_f at time $t-\gamma$ and remains in the failure set δ^n_f longer than γ can be calculated as:

$$\boldsymbol{p}^n(t-\gamma) \cdot \begin{bmatrix} \boldsymbol{I}_{|\delta^n_w|\times|\delta^n_w|} \\ \boldsymbol{0}_{|\delta^n_f|\times|\delta^n_w|} \end{bmatrix} \cdot \boldsymbol{A}^n_{wf} \cdot \left(\boldsymbol{H}^n_{fw}(\infty) - \boldsymbol{H}^n_{fw}(\gamma) \right) \tag{17}$$

Calculating the integral of the probability density in Eq. (17) from $\gamma = 0$ to $\gamma = D_b$ and multiplying the working probability of the backup battery, the probability of *Situation 2* is obtained:

$$Prob(Situation\ 2) = \int_0^{D_b} \boldsymbol{p}^n(t-\gamma) \cdot \begin{bmatrix} \boldsymbol{I}_{|\delta^n_w|\times|\delta^n_w|} \\ \boldsymbol{0}_{|\delta^n_f|\times|\delta^n_w|} \end{bmatrix} \cdot \boldsymbol{A}^n_{wf} \cdot (\boldsymbol{H}^n_{fw}(\infty) - \boldsymbol{H}^n_{fw}(\gamma)) \cdot \mathbf{1}_{|\delta^n_w|\times 1}\, d\gamma \cdot p^b_{ba} \tag{18}$$

We combine *Situation 1* and *Situation 2* to obtain $X^b_{base}(t)$'s working probability. Then, let $t \to \infty$ to obtain BS b's availability index. The derivation details can be found in Appendix B. The result is:

$$\begin{aligned} Avail^b_{base} = \boldsymbol{p}^n(0) \cdot exp(\boldsymbol{A}^n_{agg}\infty) \cdot \left(\begin{bmatrix} \mathbf{1}_{|\delta^n_w|\times 1} \\ \mathbf{0}_{|\delta^n_f|\times 1} \end{bmatrix} + \begin{bmatrix} \boldsymbol{I}_{|\delta^n_w|\times|\delta^n_w|} \\ \boldsymbol{0}_{|\delta^n_f|\times|\delta^n_w|} \end{bmatrix} \right. \\ \cdot \boldsymbol{A}^n_{wf} \cdot \left(\frac{1}{\boldsymbol{A}^n_{ff}} \right)^2 \cdot \left(\boldsymbol{I} - exp\left(\boldsymbol{A}^n_{ff} D_b \right) \right) \\ \left. \cdot \boldsymbol{A}^n_{fw} \cdot \mathbf{1}_{|\delta^n_w|\times 1} \cdot p^b_{ba} \right) \end{aligned} \tag{19}$$

where $exp(\boldsymbol{A}^n_{agg}\infty)$ is defined as $\lim_{t\to\infty} exp(\boldsymbol{A}^n_{agg}t)$.

C. Approximation and Simplification

Although Section IV-B deducts an analytical formula for the BS availability index in the distribution networks, it is difficult for further applications because of the high computational burden. Since all possible combinations of lines' status are included in $X^n_{agg}(t)$'s state space, there are up to $2^{|\phi^n_{line}|}$ states. The BS availability index (Eq. (19)) in a large distribution system cannot be calculated within an acceptable time. Approximation and simplification are needed.

1) Approximating the State Space of the Aggregated Markov Process: In $X^n_{agg}(t)$'s state space, the probabilities of different states vary. Since lines in the distribution networks have low failure rates (considering sustained interruptions) and high reliability, situations in which several lines become out of service simultaneously rarely occur. Accordingly, most of the states have rare probabilities. In power system reliability and security analysis, considering "N-k" contingencies is a common method to balance accuracy and complexity. In this paper, we adopt this method to approximate $X^n_{agg}(t)$. When constructing $X^n_{agg}(t)$'s state space, we incorporate the states that are less severe than "N-k" contingencies. Moreover, the approximation will result in a conservative estimation of the BS availability index. This is because some potential working states of $X^n_{agg}(t)$ are ignored when calculating the working probability.

2) Simplifying the Calculation of the Steady-State Probability Vector: In Section IV-A, we use $\boldsymbol{p}^n(0) \cdot \boldsymbol{P}^n_{agg}(\infty)$ to obtain the steady-state probability vector $\boldsymbol{p}^n(\infty)$, but the calculation of $exp(\boldsymbol{A}^n_{agg}\infty)$ is time consuming. Although $X^n_{agg}(t)$'s state space has been approximated, the dimension of $\boldsymbol{A}^n_{agg}$ is still large for matrix calculation. However, the steady-state probability vector $\boldsymbol{p}^n(\infty)$ can be directly calculated as follows.

For every line with failure rate λ_m and repair rate μ_m, the availability index can be calculated as:

$$Avail^m_{line} = \frac{\mu_m}{\lambda_m + \mu_m} \tag{20}$$

To calculate the i-th component of $\boldsymbol{p}^n(\infty)$, denote the corresponding binary code of state i as $x_1 x_2 \cdots x_{|\phi^n_{line}|}$, where the m-th bit x_m represents line m's state. $\boldsymbol{p}^n(\infty)(i)$ equals:

$$\boldsymbol{p}^n(\infty)(i) = \prod_{m\in\phi^n_{line}} \left(Avail^m_{line} \right)^{x_m} \left(1 - Avail^m_{line} \right)^{(1-x_m)} \tag{21}$$

This simplification avoids the calculation of $exp(\boldsymbol{A}^n_{agg}\infty)$, which decreases the computational burden for obtaining the BS availability index.

V. Base Station Dispatchable Capacity Evaluation

In this section, we first evaluate the backup duration D_b needed for the availability requirement, where the analytical formula established in Section IV is applied. Then, we calculate the minimum reserved energy capacity $R_b(t)$ by combining the required backup duration and the communication traffic data. Therefore, the dispatchable capacity can be obtained. In this paper, the dispatchable capacity comprises two parts: the energy capacity and the power capacity. The energy capacity is determined by the minimum reserved energy capacity $R_b(t)$ and the installed battery energy capacity C_b; the power capacity is determined by the rated power of power supply devices S_b and the power load of BS L_b.

The analytical relationship between the availability index $Avail^b_{base}$ and the backup duration D_b is expressed by Eq. (19). The relationship is complex. It is difficult to directly calculate the minimum backup duration needed for the availability requirement according to the equation. However, with a

required availability, the backup duration can be evaluated using the Newton-Raphson method:

Denote Eq. (19) as $Avail^{b}_{base} = f(D_b; \Omega_b)$, where D_b is the backup duration and Ω_b indicates the related distribution network parameters. The required availability index is $Avail^{req}_{base}$. Initialize the backup duration as $D_b^{(0)}$ and calculate the corresponding availability index $f(D_b^{(0)}; \Omega_b)$. The backup duration with the required availability level is calculated in an iterative manner. The iteration formation is:

$$\Delta D_b^{(k)} = -\frac{1}{f'\left(D_b^{(k)}; \Omega_b\right)}\left(Avail^{req}_{base} - f\left(D_b^{(k)}; \Omega_b\right)\right) \quad (22)$$

The minimum reserved energy capacity $R_b(t)$ is calculated using Eq. (1) and Eq. (2). It should be noted that for simplicity, we assume that the BS communication traffic is known beforehand. Further research could investigate the communication traffic forecast methods and incorporate the forecast into the proposed framework.

Based on the minimum reserved energy capacity $R_b(t)$, the BS dispatchable capacity is established:

$$\underline{SoC_b(t)} = R_b(t) \quad (23)$$

$$\overline{SoC_b(t)} = C_b \quad (24)$$

$$\overline{p^c_b(t)} = S_b - L_b(t) \quad (25)$$

$$\overline{p^d_b(t)} = L_b(t) \quad (26)$$

Eq. (23) and (24) correspond to the energy capacity. The backup battery's SoC of a BS can be dispatched in the range of $(\underline{SoC_b(t)}, \overline{SoC_b(t)})$. The available charging capacity is $\overline{SoC_b(t)} - \underline{SoC_b(t)}$; while the available discharging capacity is $\overline{SoC_b(t)} - SoC_b(t)$. Eq. (25) and (26) correspond to the power capacity. When charging, the maximum load consumption $\overline{p^c_b(t)} + L_b(t)$ of a BS should be lower than the rated power of power supply devices S_b. When discharging, the minimum load consumption $-\overline{p^d_b(t)} + L_b(k)$ of a BS is nonnegative because for most BSs injecting power back to the distribution network is prohibited. Their power converter system cannot convert the DC power in the BSs to AC power.

After the BS dispatchable capacity evaluation, we also illustrate the application: dispatching the batteries to participate in the daily optimization with the objective of minimizing the total BS operation cost. The model details can be found in Appendix C.

VI. Case Studies

Case studies are conducted on the IEEE 33-node system and the modified RBTS system to test the performance and effectiveness of the proposed framework. First, the method for calculating the availability index is analyzed. Next, the minimum backup duration calculation is studied. The dispatchable capacity is evaluated for each BS. Then, the dispatchable capacity is applied in a daily optimization scenario for illustration. Finally, the scalability of the proposed method is validated.

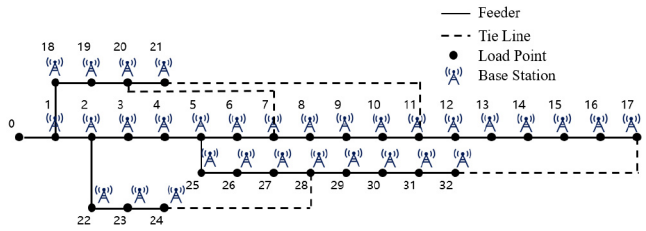

Fig. 4. The IEEE 33-node system's topology.

A. Availability Indices Calculation

The IEEE 33-node system has one main supply point and 32 load points. There are 32 feeder sections in the system, and we consider four tie-lines (node #7-#20, #11-#21, #17-#32, and #24-#28). The system data can be accessed from [29]. The system topology is shown in Fig. 4. At each node point, a 5G BS is installed for communication service. Every BS is equipped with a backup battery module. The installed energy capacity of a backup battery module is designed to serve the BS rated power load for at most three hours. The battery reliability level is 99% in the case study. The availability requirement is set as 99.999% following the NGMN standard [4].

The stochastic models are built according to Section III. We use the proposed method in Section IV to calculate the BS availability indices. The detailed results that include all BSs' availability indices with different backup duration D_b can be found in Table I. As the results show, without backup batteries ($D_b = 0$), all BSs' availability indices are lower than the requirement. This is because, on this occasion, the BSs' power load can only be supplied by the distribution networks. Moreover, BSs installed at different load points have different availability indices. For load points that are close to the main supply point (node #0), for example, node #1, the indices are relatively high; for load points that are far from the main supply point, for example, node #17, the indices are relatively low.

When backup batteries are considered, the indices ascend significantly. If the backup duration D_b is set as $3h$, all BSs' availability indices would exceed the requirement. Another phenomenon is that, with the increase of backup duration, the marginal reliability enhancement effect decreases. The improvement from $D_b = 0h$ to $D_b = 1h$ is much greater than that from $D_b = 1h$ to $D_b = 3h$. Furthermore, if backup batteries are considered, the availability indices of different BSs are similar. It is because the test system has four tie-lines. Therefore all BSs have multiple power supply paths, and their availability indices are close.

B. Minimum Backup Duration Calculation

For each BS, we evaluate the minimum backup duration needed to satisfy the requirement using the method in Section V. Fig. 5 shows the results with different battery reliability levels. When the battery reliability level is 100%, i.e., the battery failures are not considered, the minimum backup duration needed is the shortest. The average duration is 2.45 hours. With the decrease of the battery reliability level, a longer backup duration is needed for each BS to reach the availability

TABLE I
BS AVAILABILITY INDICES WITH DIFFERENT BACKUP DURATIONS IN 33-NODE SYSTEM (%)

D_b \ Node	1	2	3	4	5	6	7	8	9	10	11
0 h	99.9974	99.9833	99.9729	99.9620	99.9386	99.9833	99.9130	99.8836	99.8539	99.8483	99.8376
1 h	99.9982	99.9982	99.9982	99.9982	99.9982	99.9982	99.9982	99.9982	99.9982	99.9982	99.9982
3 h	99.9992	99.9992	99.9992	99.9992	99.9992	99.9992	99.9992	99.9992	99.9992	99.9992	99.9992
D_b \ Node	12	13	14	15	16	17	18	19	20	21	22
0 h	99.7958	99.7804	99.7636	99.7423	99.7423	99.6951	99.9927	99.9498	99.9381	99.9179	99.9704
1 h	99.9982	99.9981	99.9981	99.9981	99.9981	99.9981	99.9982	99.9982	99.9982	99.9982	99.9982
3 h	99.9992	99.9992	99.9992	99.9992	99.9992	99.9992	99.9992	99.9992	99.9992	99.9992	99.9992
D_b \ Node	23	24	25	26	27	28	29	30	31	32	
0 h	99.9448	99.9193	99.9328	99.9247	99.8945	99.8716	99.8572	99.8294	99.8206	99.8108	
1 h	99.9982	99.9982	99.9982	99.9982	99.9982	99.9982	99.9982	99.9982	99.9981	99.9981	
3 h	99.9992	99.9992	99.9992	99.9992	99.9992	99.9992	99.9992	99.9992	99.9992	99.9992	

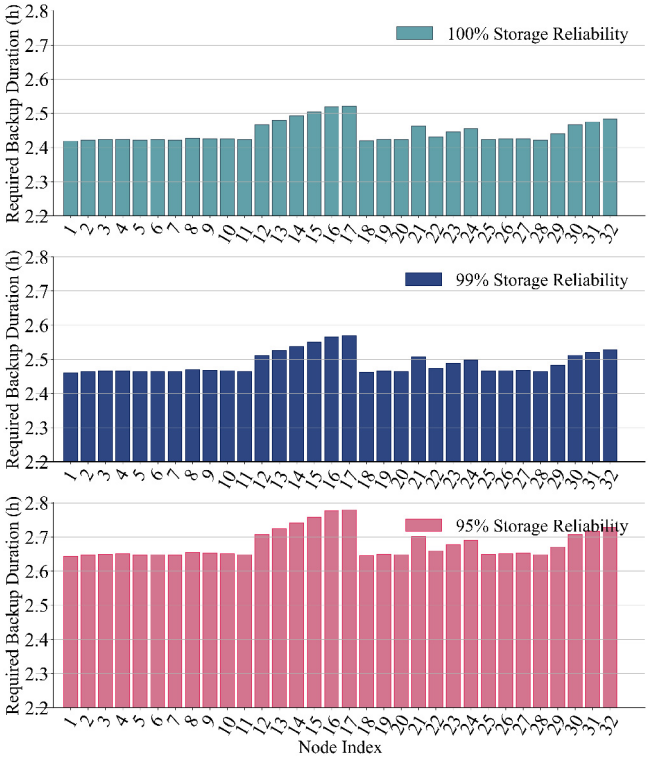

Fig. 5. Minimum backup duration for the availability requirement with different storage reliability levels.

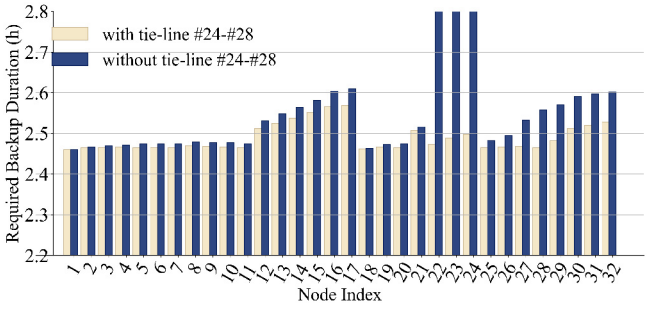

Fig. 6. Minimum backup duration for the availability requirement with different topology.

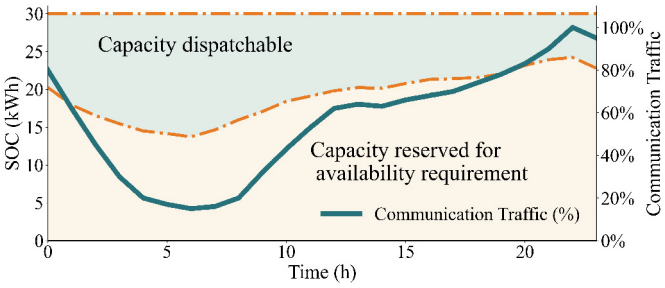

Fig. 7. BS #1's dispatchable capacity and communication traffic.

requirement. When the battery reliability level declines to 95%, the average duration increases to 2.68 hours.

In comparison with the previous results, we note that BSs installed at load points with lower availability indices require longer backup durations. The BS installed at node #17 necessitates the longest backup duration to satisfy the availability requirement. The longer backup duration the BS needs, the smaller the dispatchable capacity is.

Further, we study the influence of system topology changes. We remove the tie-line #24-#28 and re-evaluate the minimum backup duration for each BS to satisfy the availability requirement. The results are shown in Fig. 6. Removing the tie-line #24-#28 does not influence the power supply path of node #1, so the corresponding BS's minimum backup duration remains the same. For node #2∼#21 and #25∼#32, potential power supply paths decrease because of the topology change. Hence, the minimum backup duration should increase. For node #22∼#24, there is only one power supply path after removing the tie-line #24-#28. If a failure occurs on the path, these nodes cannot be restored to other feeders. Therefore, to reach the requirement, BSs installed at these nodes need 7.25, 10.56, and 12.77 hours of backup duration, respectively, which is much longer than the initially designed duration (three hours).

C. Dispatchable Capacity Evaluation and Application

Based on the obtained minimum backup duration, we can evaluate the dispatchable capacity for each BS according to Section V. The rated power of every BS communication device is set as 10 kW. The parameters of BS power consumption characteristics (Eq. (1)) and the communication traffic are taken from [22] and [30], respectively. For each BS, the power source capacity is 12 kW; the backup battery module's rated power and total energy capacity are 10 kW and 30 kWh, respectively. Fig. 7 visualizes BS #1's dispatchable capacity

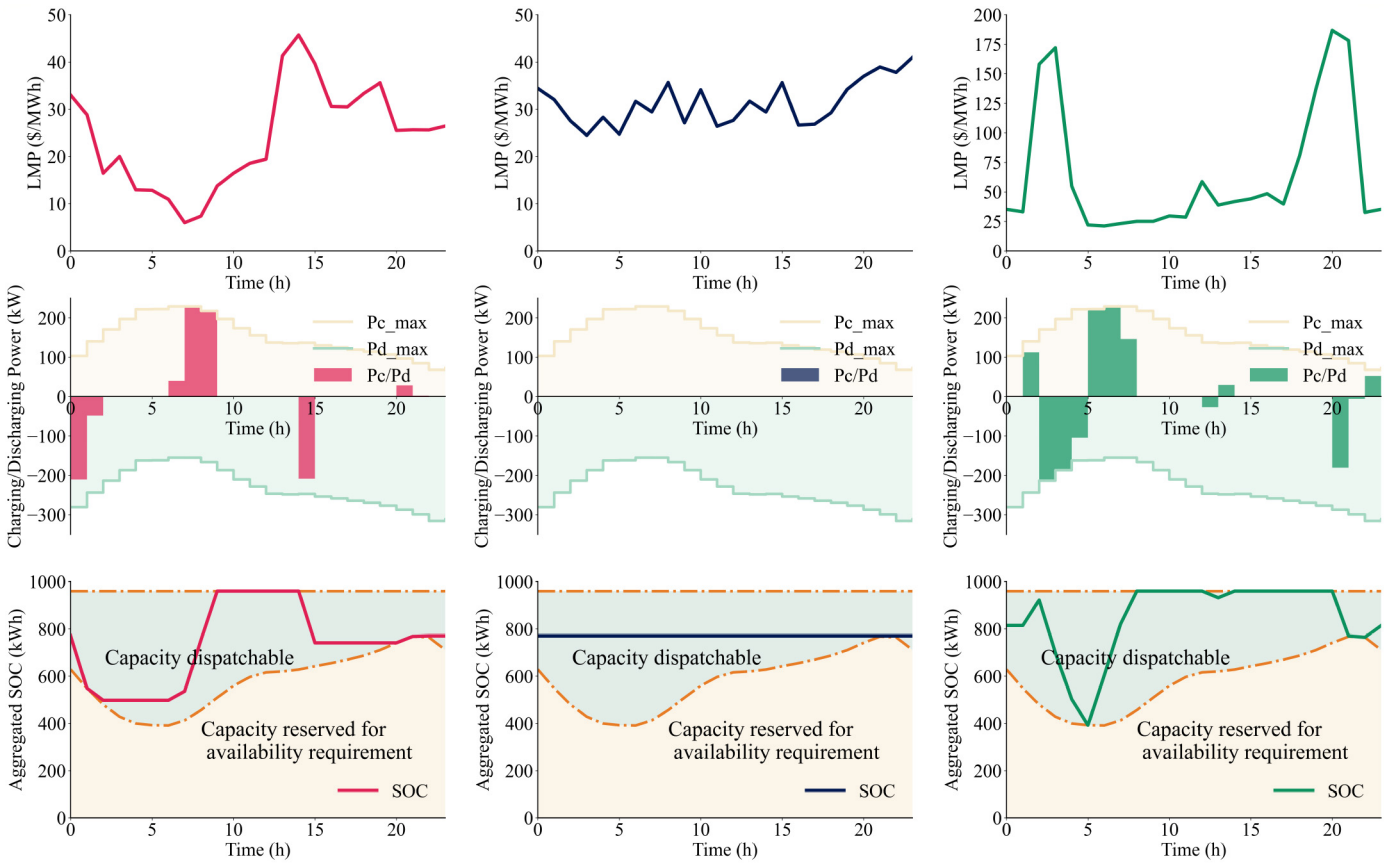

(a) Scenario 1 (b) Scenario 2 (c) Scenario 3

Fig. 8. BSs dispatch results in different scenarios.

and communication traffic. As analyzed before, two factors dominate the BS dispatchable capacity: one is the backup duration needed; the other is the communication traffic. During the communication-busy hours (e.g., hour 23), the BS power consumption is high, and more reserved energy capacity is needed. Accordingly, the dispatchable capacity is relatively small. In contrast, in communication-leisure hours (e.g., hour 6), the backup batteries are more dispatchable.

The BS dispatchable capacity is used to participate in the daily dispatch. The optimization model details can be found in Appendix C. The IEEE 33-node system is with a 3.715 MW peak active power load and 2.3 MVar peak reactive power load. The BS power consumption accounts for 7.5% of the total load. The electricity prices in different time slots are set according to the locational marginal prices (LMP) of the U.S. Southwest Power Pool (node ID: WRBEMISLD3).

We conduct a year-round operation simulation using the LMP in 2018 and take three representative scenarios for analysis. Scenario 1 is on January 10th, 2018; scenario 2 is on June 26th, 2018; and scenario 3 is on October 10th, 2018. The operation cost of dispatching BS backup batteries is compared with the cost that does not dispatch these batteries in Table II. Here, the operation cost consists of the energy consumption bills and the battery degradation cost. The detailed dispatch results are shown in Fig. 8. In the figure, the first row shows the LMP, the second row shows the backup batteries' aggregated charge/discharge power, and the third row shows the aggregated SoC curve of all BS backup batteries. Scenario 1 is a normal situation in which the LMP varies with time, and the peak-valley difference exists. As in Fig. 8(a), while maintaining the power supply reliability, the backup batteries charge at low prices and discharge at high prices. Therefore, BSs can make the temporal arbitrage with price differences. Scenario 2 represents the days when the LMP is relatively flat. In this scenario, the backup batteries are not dispatched (Fig. 8(b)) because the profits earned by temporal arbitrage cannot cover the degradation cost. Scenario 3 represents the situations when congestion occurs at the studied node. There are significant price differences between the congestion time

TABLE II
OPERATION COST OF THE BSS IN DIFFERENT SCENARIOS ($)

	Non-Dispatch	Dispatch			
	Operation Cost	Energy Cost	Degradation Cost	Operation Cost	Reduce Rate
Scenario 1	144.39	130.74	8.17	138.91	3.80%
Scenario 2	179.51	179.51	0	179.51	0%
Scenario 3	381.54	293.66	12.53	306.19	19.75%
Year Average	202.57	181.80	6.47	188.27	4.45%

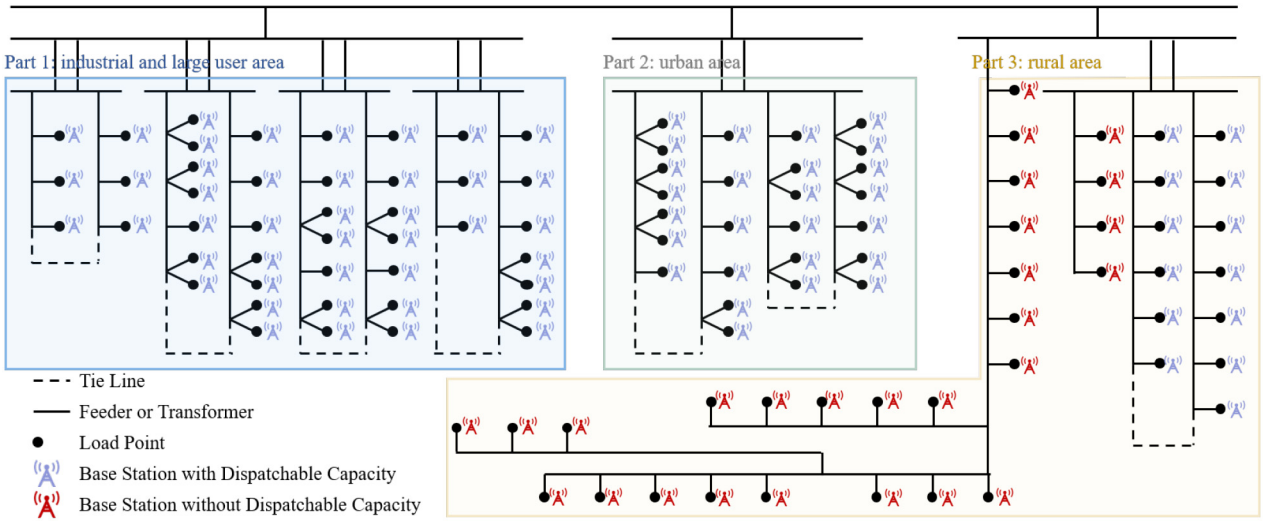

Fig. 9. BSs with/without dispatchable capacity in the modified RBTS system.

slots and the normal time slots. Hence, as in Fig. 8(c), charging at low prices and discharging at high prices can save more electricity bills. The average operation cost of the whole year is calculated in Table II to evaluate the overall performances. The results show that dispatching the BS backup batteries can reduce the average operation cost by 4.45%.

D. Scalability Test

To test the scalability of the proposed method and further investigate the impact of the distribution topology, the modified RBTS system [31] is studied. The distribution network has 110 load points, 103 feeder sections, 99 distribution transformers, and 7 tie-lines. There are three areas in the distribution network. Part 1 is the industrial and large user area. Part 2 is the urban area. Part 3 is the rural area. The detailed information can be accessed from [29]. It is assumed that there is a 5G BS installed at each load point. Every BS is equipped with a battery module whose installed capacity can serve the BS for 3 hours. The required availability is also set as 99.999%.

We evaluate the minimum backup duration every BS needed to satisfy the availability requirement. The results are shown in Fig. 9. In the system, there are 83 BSs that can reach the requirement with a backup duration of shorter than 3 hours. The average minimum backup duration of these 83 BSs is 1.94 hours. Hence, part of these BSs' installed battery capacity is dispatchable. However, 27 BSs cannot reach the requirement even when their backup duration is 3 hours. As in Fig. 9, these BSs are deployed at feeders in the rural area. These feeders are radial without tie-lines. Load points are supplied in a series way, so their power supply reliability is lower than urban load points. BSs, even with a full 3-hour backup duration, cannot satisfy the availability requirement. Indeed, BSs deployed in rural areas usually need more backup equipment such as diesel generators to deal with the relatively high probability of power supply failures. In contrast, urban distribution networks generally have tie-lines (as shown in the test system). The tie-lines can restore load points from a feeder to another feeder. Therefore, when a failure occurs on a feeder, BSs can use the backup batteries to provide UPS during the restoration. After the restoration is completed, BSs get the power supply from another intact feeder. The combination of tie-lines and backup batteries can significantly improve the power supply reliability of BSs. Our proposed method shows these backup batteries have spare capacity that is dispatchable for power systems.

VII. Discussion and Future Works

The numerical analysis demonstrates that the BSs have the dispatchable capacity that can be utilized by power systems. First, the BS availability index calculation is tested. The results show that the BS availability indices vary with different distribution network topology and different backup duration. Secondly, the minimum backup duration needed to reach the availability requirement is quantified. The numerical results prove that the minimum backup duration is affected by the reliability of the distribution network and the backup battery. By combining the minimum backup duration and the 5G BS operation characteristics, the dispatchable capacity is obtained for each BS. Case studies show that the BSs deployed at high-reliability load points (such as urban areas) have room to be dispatched. In contrast, BSs deployed at low-reliability load points (such as rural areas) do not have the dispatchable capacity, and extra backup equipment is needed. Finally, for those BSs with the dispatchable capacity, dispatching the backup batteries to participate in the daily optimization can reduce the BS operation cost.

The BS backup batteries have various potential applications in power systems. By evaluating the dispatchable capacity, the feasible operation region which meets the BS availability requirement is obtained for each backup battery module. Then, a BS backup battery can be regarded as a distributed storage resource with time-varying capacity. Although the capacity of a single BS backup battery is small for power systems, the number of BSs in the communication system is enormous, especially for 5G. The total energy storage capacity is considerable. With renewable energy development, power systems

need much more flexibility resources, so battery energy storage is becoming increasingly important. Aggregating the backup batteries in BSs can provide massive energy storage capacity as flexibility resources. Therefore, future research is needed to investigate the technologies and market mechanism design to aggregate the BS backup batteries and participate in the power system operation. These batteries can help power systems deal with the challenges of renewable energy integration in different time scales, from hours to seconds. Potential applications include peak shaving, congestion management, frequency regulation, etc.

Dispatching BS backup batteries also shortens the battery lifespan. Therefore, degradation cost is one of the inevitable factors that need to be considered. However, with technical development, battery prices have been going down rapidly in recent years. According to Bloomberg's research, battery pack prices have dropped below \$100/kWh for the first time in 2020 in China. Moreover, installing retired electric vehicle batteries in BSs for second use is the future trend, which will further reduce the equivalent degradation cost. As the battery prices fall continuously, the influence of degradation cost will decrease correspondingly.

VIII. Conclusion

BS backup batteries have the potential to improve power system operation flexibility. This paper builds a framework to evaluate the BS dispatchable capacity. The dispatchable capacity is determined by the reliability level of distribution networks and batteries under a given availability requirement. Therefore, BSs deployed at different load points have different dispatchable capacity. BSs with more reliable power supplies have more dispatchable capacity. Moreover, the dispatchable capacity of a BS varies with time. In communication-leisure hours, the backup batteries are more dispatchable. In this paper, an application of the dispatchable capacity is also illustrated: participating in the daily operation optimization. Case study results show that dispatching the backup batteries can reduce the operation cost while satisfying the availability requirement. Based on the dispatchable capacity evaluation, further research is needed to investigate the technologies and market mechanism design to aggregate the BS backup batteries and participate in the power system operation.

Appendix A
Calculation Details of the Load Point Availability Index

The probability vector $\boldsymbol{p}^n(t)$ of $X^n_{agg}(t)$ can be calculated according to the transition probability matrix $\boldsymbol{P}^n_{agg}(t)$ and the initial probability $\boldsymbol{p}^n(t)$:

$$\boldsymbol{p}^n(t) = \boldsymbol{p}^n(0) \cdot \boldsymbol{P}^n_{agg}(t) \tag{27}$$

where the transition probability matrix $\boldsymbol{P}^n_{agg}(t)$ can be expressed by:

$$\boldsymbol{P}^n_{agg}(t) = exp\left(\boldsymbol{A}^n_{agg} t\right) \tag{28}$$

We divide vector $\boldsymbol{p}^n(t)$ into two subvectors according to $X^n_{agg}(t)$'s state space indexing rule:

$$\boldsymbol{p}^n(t) = \left[\boldsymbol{p}^n_w(t), \boldsymbol{p}^n_f(t)\right] \tag{29}$$

Then, $X^n_{node}(t)$'s working probability in Eq. (7) can be rewritten as:

$$Prob\left(X^n_{node}(t) = 1\right) = \boldsymbol{p}^n_w(t) \cdot \mathbf{1}_{|\delta^n_w|\times 1} = \boldsymbol{p}^n(t) \cdot \begin{bmatrix} \mathbf{1}_{|\delta^n_w|\times 1} \\ \mathbf{0}_{|\delta^n_f|\times 1} \end{bmatrix} \tag{30}$$

We substitute the $\boldsymbol{p}^n(t)$ in Eq. (30) by Eq. (27) and Eq. (28):

$$\begin{aligned} Prob\left(X^n_{node}(t) = 1\right) &= \boldsymbol{p}^n(t) \cdot \begin{bmatrix} \mathbf{1}_{|\delta^n_w|\times 1} \\ \mathbf{0}_{|\delta^n_f|\times 1} \end{bmatrix} \\ &= \boldsymbol{p}^n(0) \cdot \boldsymbol{P}^n_{agg}(t) \cdot \begin{bmatrix} \mathbf{1}_{|\delta^n_w|\times 1} \\ \mathbf{0}_{|\delta^n_f|\times 1} \end{bmatrix} \\ &= \boldsymbol{p}^n(0) \cdot exp(\boldsymbol{A}^n_{agg} t) \cdot \begin{bmatrix} \mathbf{1}_{|\delta^n_w|\times 1} \\ \mathbf{0}_{|\delta^n_f|\times 1} \end{bmatrix} \end{aligned} \tag{31}$$

According to the definition of availability, let $t \to \infty$ to obtain the availability index $Avail^n_{node}$:

$$\begin{aligned} Avail^n_{node} &= \lim_{t\to\infty} Prob\left(X^n_{node}(t) = 1\right) \\ &= \boldsymbol{p}^n(0) \cdot exp\left(\boldsymbol{A}^n_{agg}\infty\right) \cdot \begin{bmatrix} \mathbf{1}_{|\delta^n_w|\times 1} \\ \mathbf{0}_{|\delta^n_f|\times 1} \end{bmatrix} \end{aligned} \tag{32}$$

where $exp(\boldsymbol{A}^n_{agg}\infty)$ is defined as $\lim_{t\to\infty} exp(\boldsymbol{A}^n_{agg} t)$.

Appendix B
Calculation Details of the Base Station Availability Index

A. Calculation of $\boldsymbol{h}^n_{fw}(\tau)$ and $\boldsymbol{H}^n_{fw}(\tau)$

According to Eq. (9), $\boldsymbol{P}^n_{ff}(\tau)$ represents the probability that the Markov chain only jumps in the failure set δ^n_f and does not enter the working set δ^n_w in time interval τ; $\boldsymbol{A}^n_{fw}$ represents the probability density that the Markov chain jumps from the failure set δ^n_f to the working set δ^n_w. Thus, $\boldsymbol{h}^n_{fw}(\tau)$ can be calculated as follows [21]:

$$\boldsymbol{h}^n_{fw}(\tau) = \boldsymbol{P}^n_{ff}(\tau) \cdot \boldsymbol{A}^n_{fw} \tag{33}$$

where $\boldsymbol{P}^n_{ff}(\tau)$ is obtained by [32]:

$$\boldsymbol{P}^n_{ff}(t) = exp\left(\boldsymbol{A}^n_{ff} t\right) \tag{34}$$

Then, $\boldsymbol{H}^n_{fw}(\tau)$ can be calculated by integration:

$$\begin{aligned} \boldsymbol{H}^n_{fw}(\tau) &= \int_0^\tau \boldsymbol{h}^n_{fw}(x)dx \\ &= \int_0^\tau \boldsymbol{P}^n_{ff}(\tau) \cdot \boldsymbol{A}^n_{fw} dx \\ &= \int_0^\tau exp\left(\boldsymbol{A}^n_{ff} x\right) \cdot \boldsymbol{A}^n_{fw} dx \\ &= \frac{1}{\boldsymbol{A}^n_{ff}} \cdot \left(exp(\boldsymbol{A}^n_{ff}\tau) - \boldsymbol{I}\right) \cdot \boldsymbol{A}^n_{fw}. \end{aligned} \tag{35}$$

B. Calculation of the Base Station Availability Index

Combining Eq. (7) and Eq. (18), BS b's working probability is:

$$\begin{aligned} &Prob(\text{BS } b \text{ is working at } t) \\ &= \boldsymbol{p}^n(t) \cdot \begin{bmatrix} \mathbf{1}_{|\delta_w^n|\times 1} \\ \mathbf{0}_{|\delta_f^n|\times 1} \end{bmatrix} \\ &\quad + \int_0^{D_b} \boldsymbol{p}^n(t-\gamma) \cdot \begin{bmatrix} \boldsymbol{I}_{|\delta_w^n|\times|\delta_w^n|} \\ \mathbf{0}_{|\delta_f^n|\times|\delta_w^n|} \end{bmatrix} \cdot \boldsymbol{A}_{wf}^n \\ &\quad \cdot \left(\boldsymbol{H}_{fw}^n(\infty) - \boldsymbol{H}_{fw}^n(\gamma)\right) \cdot \mathbf{1}_{|\delta_w^n|\times 1}\, d\gamma \cdot p_{ba}^b \end{aligned} \tag{36}$$

where $\boldsymbol{H}_{fw}^n(\infty)$ is defined as $\lim_{t\to\infty} \boldsymbol{H}_{fw}^n(t)$.

According to the definition of availability, let $t \to \infty$ to obtain the availability index. The availability $Avail_{base}^b$ is:

$$\begin{aligned} Avail_{base}^b &= \lim_{t\to\infty} Prob(\text{BS } b \text{ is working at } t) \\ &= \boldsymbol{p}^n(\infty) \cdot \begin{bmatrix} \mathbf{1}_{|\delta_w^n|\times 1} \\ \mathbf{0}_{|\delta_f^n|\times 1} \end{bmatrix} + \int_0^{D_b} \boldsymbol{p}^n(\infty) \cdot \begin{bmatrix} \boldsymbol{I}_{|\delta_w^n|\times|\delta_w^n|} \\ \mathbf{0}_{|\delta_f^n|\times|\delta_w^n|} \end{bmatrix} \\ &\quad \cdot \boldsymbol{A}_{wf}^n \cdot (\boldsymbol{H}_{fw}^n(\infty) - \boldsymbol{H}_{fw}^n(\gamma)) \cdot \mathbf{1}_{|\delta_w^n|\times 1}\, d\gamma \cdot p_{ba}^b \\ &= \boldsymbol{p}^n(\infty) \cdot \begin{bmatrix} \mathbf{1}_{|\delta_w^n|\times 1} \\ \mathbf{0}_{|\delta_f^n|\times 1} \end{bmatrix} + \boldsymbol{p}^n(\infty) \cdot \begin{bmatrix} \boldsymbol{I}_{|\delta_w^n|\times|\delta_w^n|} \\ \mathbf{0}_{|\delta_f^n|\times|\delta_w^n|} \end{bmatrix} \cdot \boldsymbol{A}_{wf}^n \\ &\quad \cdot \int_0^{D_b} \frac{1}{\boldsymbol{A}_{ff}^n} \cdot (-exp(\boldsymbol{A}_{ff}^n \gamma)) \cdot \boldsymbol{A}_{fw}^n \cdot \mathbf{1}_{|\delta_w^n|\times 1}\, d\gamma \cdot p_{ba}^b \\ &= \boldsymbol{p}^n(\infty) \cdot \begin{bmatrix} \mathbf{1}_{|\delta_w^n|\times 1} \\ \mathbf{0}_{|\delta_f^n|\times 1} \end{bmatrix} + \boldsymbol{p}^n(\infty) \cdot \begin{bmatrix} \boldsymbol{I}_{|\delta_w^n|\times|\delta_w^n|} \\ \mathbf{0}_{|\delta_f^n|\times|\delta_w^n|} \end{bmatrix} \cdot \boldsymbol{A}_{wf}^n \\ &\quad \cdot \left(\frac{1}{\boldsymbol{A}_{ff}^n}\right)^2 \cdot (\boldsymbol{I} - exp(\boldsymbol{A}_{ff}^n D_b)) \cdot \boldsymbol{A}_{fw}^n \cdot \mathbf{1}_{|\delta_w^n|\times 1} \cdot p_{ba}^b \\ &= \boldsymbol{p}^n(0) \cdot exp\left(\boldsymbol{A}_{agg}^n \infty\right) \\ &\quad \cdot \left(\begin{bmatrix} \mathbf{1}_{|\delta_w^n|\times 1} \\ \mathbf{0}_{|\delta_f^n|\times 1} \end{bmatrix} + \begin{bmatrix} \boldsymbol{I}_{|\delta_w^n|\times|\delta_w^n|} \\ \mathbf{0}_{|\delta_f^n|\times|\delta_w^n|} \end{bmatrix} \cdot \boldsymbol{A}_{wf}^n \cdot \left(\frac{1}{\boldsymbol{A}_{ff}^n}\right)^2 \right. \\ &\quad \left. \cdot (\boldsymbol{I} - exp(\boldsymbol{A}_{ff}^n D_b)) \cdot \boldsymbol{A}_{fw}^n \cdot \mathbf{1}_{|\delta_w^n|\times 1} \cdot p_{ba}^b \right) \end{aligned} \tag{37}$$

where $\boldsymbol{p}^n(\infty)$ is the steady-state probability vector, and $exp(\boldsymbol{A}_{agg}^n \infty)$ is defined as $\lim_{t\to\infty} exp(\boldsymbol{A}_{agg}^n t)$.

APPENDIX C
DAILY DISPATCH MODEL OF THE DISTRIBUTION NETWORK

We illustrate an application scenario to show the proposed framework's effectiveness: dispatching the backup batteries to participate in the daily optimization. It should be noted that the symbol system of the Appendix is different from that of the main body.

The objective function is to minimize the total BS operation cost:

$$min\ C = C_{pur} + C_{shed} + C_{deg} \tag{38}$$

where C_{pur} is the energy cost, C_{shed} is the load shedding cost, and C_{deg} is the battery degradation cost. C_{pur} and C_{shed} are calculated as follows:

$$C_{pur} = \sum_b \sum_k \pi_k P_b(k) \tag{39}$$

$$C_{shed} = \sum_b \sum_k \pi_s P_b^s(k) \tag{40}$$

where π_k is the electricity price at time slot k, and π_s is the load shedding price; $P_b(k)$ is the power consumption of BS b at time slot k; $P_b^s(k)$ is the load shedding of BS b at time slot k. This paper adopts the lithium-ion battery degradation cost model in [33] to calculate the degradation cost since the lithium-ion batteries are the future trend providing BS UPS. In the model [33], the degradation cost is proportional to the amount of battery charging/discharging. Therefore, the degradation cost of BS b at time slot k is:

$$C_{deg}^b(k) = \lambda_b (p_b^c(k) + p_b^d(k)) \tag{41}$$

where λ_b is the linearized battery degradation cost co-efficient, and $p_b^c(k)$ and $p_b^d(k)$ are the battery charging/discharging power. λ_b is calculated by:

$$\lambda_b = \frac{\lambda_{cell}}{2N_b \overline{\Delta SoC_b}} \tag{42}$$

where λ_{cell} is the battery cell price, N_b is the number of cycles that the battery could be operated within SoC limit, and $\overline{\Delta SoC_b}$ is the deference of the upper and lower SoC limits. Hence, the total degradation cost is:

$$C_{deg} = \sum_b \sum_k C_{deg}^b(k) \tag{43}$$

The power flow equations are presented using the DistFlow model:

$$\sum_{mi} P_{mi}(k) - \sum_{ij} \left(P_{ij}(k) + R_{ij} I_{ij}(k)^2\right) = P_i(k) \tag{44}$$

$$\sum_{mi} Q_{mi}(k) - \sum_{ij} \left(Q_{ij}(k) + X_{ij} I_{ij}(k)^2\right) = Q_i(k) \tag{45}$$

$$V_i(k)^2 - V_j(k)^2 = 2\left(R_{ij}P_{ij}(k) + X_{ij}Q_{ij}(k)\right) + \left(R_{ij}^2 + X_{ij}^2\right) \times I_{ij}(k)^2 \tag{46}$$

$$I_{ij}(k)^2 V_i(k)^2 = P_{ij}(k)^2 + Q_{ij}(k)^2 \tag{47}$$

where $P_i(k)$ and $Q_i(k)$ are the active and reactive power consumption of node i at time slot k; $V_i(k)$ is the voltage magnitude of node i at time slot k; $P_{mi}(k)$ and $Q_{mi}(k)$ are the active and reactive power transfer from node m to i at time slot k; $P_{ij}(k)$ and $Q_{ij}(k)$ are the active and reactive power transfer from node i to j at time slot k; R_{ij} and X_{ij} are the resistance and the reactance of branch ij; $I_{ij}(k)$ is the current magnitude of branch ij at time slot k.

Security constraints include the voltage constraints of nodes and the current constraints of branches:

$$V_{min} \le V_i(k) \le V_{max} \tag{48}$$

$$0 \le I_{ij}(k) \le I_{ij,max} \tag{49}$$

For each node, the active power consumption can be expressed as follows:

$$P_i(k) = P_i^d(k) + \sum_{b\in\phi_{base}^i} \left(p_b^c(k) - p_b^d(k)\right) \tag{50}$$

where $P_i^d(k)$ is the load demand of node i at time slot k; $p_b^c(k)$ and $p_b^d(k)$ are the charging and discharging power of BS b

at time slot k. The load of BS equipment $(P_b(k) - P_b^s(k))$ is considered in $P_i^d(k)$.

According to the dispatchable capacity analyzed in Section V, the operation constraints of BS backup batteries are as follows:

$$\underline{SoC_b(k)} \le SoC_b(k) \le \overline{SoC_b(k)} \tag{51}$$

$$SoC_b(k+1) = SoC_b(k) + \eta_b^c \cdot p_b^c(k) - p_b^d(k)/\eta_b^d \tag{52}$$

$$0 \le p_b^c(k) \le \overline{p_b^c(k)} \cdot y_b(k) \tag{53}$$

$$0 \le p_b^d(k) \le \overline{p_b^d(k)} \cdot (1 - y_b(k)) \tag{54}$$

where η_b^c and η_b^d are the charging and discharging efficiency; $y_b(k)$ is a 0-1 variable that represents the operation status of BS b's backup battery. Eq. (51) is the SoC range constraint. Eq. (52) is the battery energy conservation equation. Eq. (53) and (54) are the charging and discharging limit constraints.

The daily dispatch optimization model includes Eq. (38)–(54). To solve, second order cone programming (SOCP) relaxation, which is widely used in distribution networks, is adopted. After the relaxation, the model is transformed into a mix-integer SOCP form.

ACKNOWLEDGMENT

The authors would like to thank Mr. Tan Gan, who is currently purchasing the Ph.D. degree with Yale University, for his valuable suggestions on stochastic process modeling and analysis.

REFERENCES

[1] C.-X. Wang *et al.*, "Cellular architecture and key technologies for 5G wireless communication networks," *IEEE Commun. Mag.*, vol. 52, no. 2, pp. 122–130, Feb. 2014.

[2] E. Dahlman *et al.*, "5G wireless access: Requirements and realization," *IEEE Commun. Mag.*, vol. 52, no. 12, pp. 42–47, Dec. 2014.

[3] I. Chih-Lin, S. Han, and S. Bian, "Energy-efficient 5G for a greener future," *Nat. Electron.*, vol. 3, no. 4, pp. 182–184, 2020.

[4] "5G white paper," Next Gener. Mobile Netw., Frankfurt, Germany, White Paper, 2015.

[5] "5G telecom power target network white paper," Amsterdam, The Netherlands, Global ICT Energy Efficiency Summit, White Paper, 2019.

[6] Y. Yoo, S. Jung, and G. Jang, "Dynamic inertia response support by energy storage system with renewable energy integration substation," *J. Mod. Power Syst. Clean Energy*, vol. 8, no. 2, pp. 260–266, 2020.

[7] Y. Sun, Z. Zhao, M. Yang, D. Jia, W. Pei, and B. Xu, "Overview of energy storage in renewable energy power fluctuation mitigation," *CSEE J. Power Energy Syst.*, vol. 6, no. 1, pp. 160–173, 2020.

[8] E. Lannoye, D. Flynn, and M. O'Malley, "Evaluation of power system flexibility," *IEEE Trans. Power Syst.*, vol. 27, no. 2, pp. 922–931, May 2012.

[9] H. Ming, B. Xia, K.-Y. Lee, A. Adepoju, S. Shakkottai, and L. Xie, "Prediction and assessment of demand response potential with coupon incentives in highly renewable power systems," *Protect. Control Mod. Power Syst.*, vol. 5, pp. 1–14, Apr. 2020.

[10] A. Chowdhury and D. Koval, *Power Distribution System Reliability: Practical Methods and Applications*, vol. 48. Hoboken, NJ, USA: Wiley, 2011.

[11] A. Arefi, G. Ledwich, G. Nourbakhsh, and B. Behi, "A fast adequacy analysis for radial distribution networks considering reconfiguration and DGs," *IEEE Trans. Smart Grid*, vol. 11, no. 5, pp. 3896–3909, Sep. 2020.

[12] K. R. Timalsena, P. Piya, and R. Karki, "A novel methodology to incorporate circuit breaker active failure in reliability evaluation of electrical distribution networks," *IEEE Trans. Power Syst.*, vol. 36, no. 2, pp. 1013–1022, Mar. 2021.

[13] Z. Li, W. Wu, B. Zhang, and X. Tai, "Analytical reliability assessment method for complex distribution networks considering post-fault network reconfiguration," *IEEE Trans. Power Syst.*, vol. 35, no. 2, pp. 1457–1467, Mar. 2020.

[14] W. Liu, Z. Lin, L. Wang, Z. Wang, H. Wang, and Q. Gong, "Analytical reliability evaluation of active distribution systems considering information link failures," *IEEE Trans. Power Syst.*, vol. 35, no. 6, pp. 4167–4179, Nov. 2020.

[15] P. Gautam, P. Piya, and R. Karki, "Development and integration of momentary event models in active distribution system reliability assessment," *IEEE Trans. Power Syst.*, vol. 35, no. 4, pp. 3236–3246, Jul. 2020.

[16] M. Jooshaki *et al.*, "Linear formulations for topology-variable-based distribution system reliability assessment considering switching interruptions," *IEEE Trans. Smart Grid*, vol. 11, no. 5, pp. 4032–4043, Sep. 2020.

[17] Y. Liu, Y. Su, Y. Xiang, J. Liu, L. Wang, and W. Xu, "Operational reliability assessment for gas-electric integrated distribution feeders," *IEEE Trans. Smart Grid*, vol. 10, no. 1, pp. 1091–1100, Jan. 2019.

[18] B. Roux and R. Sauvé, "A general solution to the time interval omission problem applied to single channel analysis," *Biophys. J.*, vol. 48, no. 1, pp. 149–158, 1985.

[19] Z. Zheng, L. Cui, and A. G. Hawkes, "A study on a single-unit Markov repairable system with repair time omission," *IEEE Trans. Rel.*, vol. 55, no. 2, pp. 182–188, Jun. 2006.

[20] X. Bao and L. Cui, "An analysis of availability for series Markov repairable system with neglected or delayed failures," *IEEE Trans. Rel.*, vol. 59, no. 4, pp. 734–743, Dec. 2010.

[21] B. Liu, L. Cui, and Y. Wen, "Interval reliability for aggregated Markov repairable system with repair time omission," *Ann. Oper. Res.*, vol. 212, no. 1, pp. 169–183, 2014.

[22] P. Frenger and R. Tano, "More capacity and less power: How 5G NR can reduce network energy consumption," in *Proc. IEEE 89th Veh. Technol. Conf. (VTC-Spring)*, 2019, pp. 1–5.

[23] *IEEE Guide for Electric Power Distribution Reliability Indices—Redline*, IEEE Standard 1366-2012, pp. 1–92, 2012.

[24] C. Chen, W. Wu, B. Zhang, and C. Singh, "An analytical adequacy evaluation method for distribution networks considering protection strategies and distributed generators," *IEEE Trans. Power Del.*, vol. 30, no. 3, pp. 1392–1400, Jun. 2015.

[25] R. Billinton and P. Wang, "Teaching distribution system reliability evaluation using Monte Carlo simulation," *IEEE Trans. Power Syst.*, vol. 14, no. 2, pp. 397–403, May 1999.

[26] R. E. Tarjan, *Data Structures and Network Algorithms*. Philadelphia, PA, USA: SIAM, 1983.

[27] R. Billinton and K. E. Bollinger, "Transmission system reliability evaluation using Markov processes," *IEEE Trans. Power App. Syst.*, vol. PAS-87, no. 2, pp. 538–547, Feb. 1968.

[28] S.-Z. Yu, "Chapter 1—Introduction," in *Hidden Semi-Markov Models*, S.-Z. Yu, Ed. Boston, MA, USA: Elsevier, 2016, pp. 1–26.

[29] P. Yong *et al. Test System for Evaluating the Dispatchable Capacity of Basestation Backup Batteries in Distribution Networks*. Accessed: Feb. 2, 2021. [Online]. Available: https://docs.google.com/spreadsheets/d/1j5oDQWDVsLQJPia9Mm8znvlawnOOKYeJjmfLm3icRhI/edit?usp=sharing

[30] G. Auer *et al.*, "Cellular energy efficiency evaluation framework," in *Proc. IEEE 73rd Veh. Technol. Conf. (VTC Spring)*, 2011, pp. 1–6.

[31] R. Billinton and S. Jonnavithula, "A test system for teaching overall power system reliability assessment," *IEEE Trans. Power Syst.*, vol. 11, no. 4, pp. 1670–1676, Nov. 1996.

[32] D. C. G. Hawkes, "On the stochastic properties of single ion channels," *Proc. Roy. Soc. London*, vol. 211, no. 1183, pp. 205–235, 1981.

[33] Y. Shi, B. Xu, D. Wang, and B. Zhang, "Using battery storage for peak shaving and frequency regulation: Joint optimization for superlinear gains," *IEEE Trans. Power Syst.*, vol. 33, no. 3, pp. 2882–2894, May 2018.

Pei Yong (Graduate Student Member, IEEE) received the B.S. degree in electrical engineering from Tsinghua University, Beijing, China, in 2018, where he is currently pursuing the Ph.D. degree.

His research interests include power system reliability evaluation, multienergy systems, renewable energy, and cellular base station managements.

Ning Zhang (Senior Member, IEEE) received the B.S. and Ph.D. degrees from Tsinghua University, Beijing, China, in 2007 and 2012, respectively.

He is currently an Associate Professor with Tsinghua University. His research interests include multiple energy systems integration, renewable energy, and power system planning and operation.

Qingchun Hou (Graduate Student Member, IEEE) received the B.S. degree from the Department of Electrical Engineering, Huazhong University of Science and Technology in 2016. He is currently pursuing the Ph.D. degree in Tsinghua University.

He was also a visiting Ph.D. student with the University of Washington. His research interests include power system operation and planning with high renewable energy penetration, data-driven analytics, power system optimization, and machine learning.

Yuxiao Liu (Graduate Student Member, IEEE) received the B.S. degree from the Electrical Engineering Department, Tsinghua University, China, in 2016, where he is currently pursuing the Ph.D. degree.

He was also a Visiting Student Researcher with the Laboratory for Information and Decision Systems, Massachusetts Institute of Technology, Cambridge, MA, USA. His research interests include data-driven power grid analysis and power system cascading failures modeling.

Fei Teng (Member, IEEE) received the B.Eng. degree in electrical engineering from Beihang University, China, in 2009, and the Ph.D. degree in electrical engineering from Imperial College London, U.K., in 2015.

He is currently a Lecturer with the Department of Electrical and Electronic Engineering, Imperial College London. His research focuses on scheduling and market design for low-inertia power system, cyber-resilient energy system operation and control, and objective-based data analytics for future energy systems.

Song Ci (Senior Member, IEEE) received the Ph.D. degree from the Department of Electrical Engineering, University of Nebraska–Lincoln, Lincoln, NE, USA, in 2002.

He is currently a Professor with the Department of Electrical Engineering, Tsinghua University, Beijing, China. His research interests include largescale dynamic complex system modeling and optimization, as well as its applications in the areas of the Internet and the energy Internet.

Chongqing Kang (Fellow, IEEE) received the Ph.D. degree from Tsinghua University, Beijing, China, in 1997.

He is currently a Professor with Tsinghua University. His research interests include power system planning, power system operation, renewable energy, low carbon electricity technology, and load forecasting.